

Utilization of Bitter orange seeds as a novel source for recovery of pectin: Compositional and rheological characterization

Mohammad Nejatian

Kermanshah University of Medical Sciences

Diako Khodaei (✉ diako.khodaei@hotmail.com)

Tarbiat Modares University

Hassan Ahmadi Gavlighi

Tarbiat Modares University

Azizollaah Zargaraan

National Nutrition and Food, Shahid Beheshti University

Research Article

Keywords: Pectin, Orange seeds, Sugar composition, Molecular weight, Rheological properties

Posted Date: July 14th, 2021

DOI: <https://doi.org/10.21203/rs.3.rs-651981/v1>

License:  This work is licensed under a Creative Commons Attribution 4.0 International License.

[Read Full License](#)

1 **Utilization of Bitter orange seeds as a novel source for recovery of pectin:**
2 **Compositional and rheological characterization**

3
4 **Mohammad Nejatian ^a, Diako Khodaei ^{b*}, Hassan Ahmadi Gavlighi ^{b*}, Azizollaah**
5 **Zargaraan^c**

6 ^a Department of Food Science and Technology, School of Nutrition Science and Food
7 Technology, Kermanshah University of Medical Sciences, Kermanshah, Iran

8 ^b Department of Food Science and Technology, Tarbiat Modares University, P.O. Box 14115-
9 336, Tehran, Iran

10 ^c Department of Food and Nutrition Policy and Planning Research, National Nutrition and Food,
11 Shahid Beheshti University, M.C., P.O. Box 19395-4741, Tehran, Iran

12
13 *Corresponding authors:

14 Dr. Diako Khodaei

15 E-mail address: diako.khodaei@hotmail.com , Tel: (+353) 089 488 8234

16 Dr. Hassan Ahmadi Gavlighi

17 E-mail address: ahmadi_ha@modares.ac.ir, Tel: (+98) 2148292313

21 **Abstract**

22 The seeds from bitter orange, a by-product from the juice making step, hold the potential to
23 facilitate novel, easy yet high quality pectin extraction. To test this hypothesis, the pectin from
24 orange seeds (OSP) were extracted by distilled water and its compositional parameters and
25 rheological behavior then evaluated. Results showed that galacturonic acid was the major
26 component of OSP (~ 425 mg/g) confirming the purity of extracted pectin, followed by glucose
27 and some minor neutral sugars. M_w , R_n and, R_z for the OSP were 4511.8 (kDa), 61 (nm), and 61.1
28 (nm), respectively. Rheological measurements showed shear-thinning behavior for OSP that by
29 increasing temperature from 5 to 45 °C, the viscosity of the gum decreased. Power law fitted as
30 the best rheological model describing the flow behavior of OSP. Strain sweep dynamic rheological
31 measurements confirmed an entangled network structure for OSP and the addition of NaCl to the
32 gum dispersion, decreased the consistency coefficient from 35.6 to 23.18 Pa.sⁿ, while the flow
33 behavior index remained unchanged. These results demonstrate for the first time that the OSP can
34 be used as a new source of pectin, with likely a wide range of applications in food industry.

35

36 **Keywords:** Pectin; Orange seeds; Sugar composition; Molecular weight; Rheological properties.

37 **1. Introduction**

38 Hydrocolloids are water-soluble biopolymers with a wide application in food industry. They are
39 commonly used to improve textural properties of food as a gelation and viscosity improving agents
40 (Nejatian et al., 2020). Pectin one of the major hydrocolloids in food processing industry is a
41 polysaccharide with 1, 4-galacturonic acid units and some of its carboxyl groups can be substituted
42 with methyl esters or amide groups (Löfgren and Hermansson, 2007). It is widely used as an
43 ingredient for providing specific textural and rheological properties to processed food as a
44 gelling/thickening agent or as an emulsion stabilizer for acidified dairy drinks (Christiaens et al.,
45 2016).

46 The source of pectin, the extraction procedures, the particle size distribution, the patterns of
47 acylation, the degree of esterification (DE) and the nature and position of the neutral sugars have
48 a great impact on the specifications of pectin from the various origins (Maxwell et al., 2012).
49 Pectin is considered as an invaluable by-product of the citrus processing industry. About 85% of
50 the globally commercial pectin is sourced from citrus waste which can be produced from fresh or
51 processed peels of lemon, grapefruit, and oranges (Berk, 2016).

52 Disadvantages associated with pectin extraction from citrus peels include the use of corrosion
53 mineral acid, high temperature and extended extraction time. Together these may affect pectin
54 quality and moreover damage equipment. Furthermore, the steps of filtration, discoloration and
55 concentration of pectin solution before alcohol precipitation are associated with both high cost and
56 use of time (May, 1990). Therefore, new sources of pectin with both lower extraction time and
57 production costs is both economically and technologically appealing (Shan, 2016). Previous
58 studies examining pectin extraction have been varied in their approach. The extraction and
59 physiochemical properties of pectin from the heads of sunflowers was studied by Peng et al. (Peng

60 et al., 2020). Asgari and co-workers (Asgari et al., 2020) studied the walnut processing waste as a
61 novel source of pectin. Gharibzahedi et al. (Gharibzahedi et al., 2019) evaluated the pectin
62 extracted from Fig (*Ficus carica* L.) skin. Chaliha and co-authors (Chaliha et al., 2018) extracted
63 pectin from *Terminalia ferdinandiana*- a native Australian fruit. Finally, the possibility of using
64 Palmyra Palm (*Borassus aethiopum* Mart.) fruit was evaluated by Assoi et al. (Assoi et al., 2017).
65 The bitter orange (*Citrus aurantium*) contains many seeds and differs from the orange by several
66 characters including the acidic pulp and bitterer albedo (Moufida and Marzouk, 2003). It is
67 commonly used for essential oils, in the perfume industry and for the production the marmalade.
68 In the Middle East, the juice of the ripen fruit can be used as a salad dressing or as a flavoring
69 (Zibae et al., 2020).

70 It is necessary to understand the rheological properties and determination of sugar composition of
71 pectin from new sources to evaluate their thickener potential. The flow behavior of hydrocolloids
72 solutions is important to assess processing parameters, textural properties of formulated foods,
73 design of unit operations and development of product engineering (Balaghi et al., 2011; Rincón et
74 al., 2014). To date there is no report on the extraction of pectin from orange seeds and hence an
75 evaluation of its compositional and functional properties. Therefore, the main objective of this
76 research was to extract and characterize the sugar composition, molecular weight, and rheological
77 properties of pectin from bitter orange seeds as a novel source of pectin.

78

79 **2. Material and methods**

80 *2.1 Materials and extraction method*

81 The bitter orange fruit (*Citrus aurantium* L.) was used in this study, collected from trees growing
82 in Mazandaran province of Iran during October and November 2020 and according to the
83 permission and the national guideline of Agricultural Research Education and Extension
84 Organization of Iran. Phenotypic identification of the specimen was done by Dr. Saeid Hazrati,
85 academic member of Shahid Madani University of Tabriz, Iran.

86 The seeds were collected from bitter oranges during the juice extraction. Seeds were washed with
87 tap water to remove the fruit pulp and drained completely to remove the excess water. Afterward,
88 the seeds soaked in distilled water (pH= 7) in a seed ratio of 6:1 at 70 ± 1 °C and stirred for 30 min
89 (solid/liquid ratio selected based on preliminary test). Thereafter, pectin coats were removed from
90 the seeds by passing through a 600 µm sieve and collected in a flask. The extracted solution mixed
91 with three volumes of 96% v/v ethanol and placed in the fridge (4 °C). After 24 h, the flocculated
92 pectin collected and dried in an oven with circulating air at 30 °C. The dehydrated pectin (OSP)
93 was pulverized with a miller, packed, and kept in cool and dry condition prior test.

94 Standards of monosaccharides (galacturonic acid, glucose, arabinose, galactose, rhamnase, and
95 fucose) and trifluoroacetic acid (TFA) with purity of $\geq 99\%$ were purchased from Merck
96 (Darmstadt, Germany).

97 *2.2 Compositional analysis*

98 AOAC method (AOAC, 2016) was used for determination of moisture content and total ash
99 content. Kjeldal method was used for the determination of total protein content with the nitrogen
100 value of 6.25 (Razavi et al., 2014).

101 After hydrolysis 4 g/l of OSP by TFA (2 M) for 2h at 121 °C, the monosaccharide composition
102 analyzed by high-performance anion-exchange chromatography with a pulsed amperometric

103 detector (DECADE Elite). Separations carried out in a CarboPac PA1(4×250mm) column (Dionex
104 Corp., Sunnyvale, CA). Samples were passed through 0.22 µm filter prior injections into the
105 column. The monosaccharides separation through the column was carried out according to the
106 method of (Gavlighi et al., 2013).

107 *2.3 Degree of esterification (DE)*

108 The titration method proposed by Chaharbaghi et al. (Chaharbaghi et al., 2017) was used for
109 determination of DE of pectin sample. To do this, 100 mg of dried powder of sample was added
110 to 2 ml of ethanol and dissolved in 20 ml deionized water at 40 °C. Afterward, 5 ml of
111 phenolphthalein reagent was added to the solution and titrated with NaOH (0.1 M). The amount
112 of NaOH used for titration recorded as V_i . Afterward, 10 ml of NaOH was added to the solution
113 and mixed for 30 min for complete hydrolysis. 10 ml of HCl (0.1 M) was introduced to the solution
114 and mixed vigorously to completely disappear the pink color. After the addition of drops of
115 phenolphthalein, the excessive amount of HCl was titrated with NaOH to obtain a pale pink color
116 and the volume of NaOH was recorded as the V_f . The DE of pectin was calculated according the
117 following equation (Hosseini et al., 2016):

$$118 \quad DE = \left(\frac{V_f}{V_i + V_f} \right) \times 100$$

119 *2.4 Determination of molecular parameters*

120 Molecular weight averages (M_n , M_w , M_z) of the OSP were determined by using a size exclusion
121 chromatography system (flow rate of 0.4 mL/min with 0.15 M NaNO_3 and 0.02% NaN_3) and
122 equipped with TSK G5000 PW column (7.5 × 600 mm; Toso Biosep, Montgomeryville, PA, USA)
123 joint to a UV detector (Waters, 2487), multi-angle laser light scattering (HELEOS; Wyatt
124 Technology Corp, Santa Barbara, CA, USA) and a refractive index detector (Waters, 2414)

125 (HPSEC-UV-MALLS-RI). Bovine serum albumin (BSA) was used as a standard for determination
126 of the volume delays among the US, MALLS, and RI detectors. ASTRA 5.3 software (Wyatt
127 Technology Corp.) applied for data acquisition and to calculate the M_w average, M_n , and M_z .

128 *2.5 Rheological Measurements*

129 In order to determine the rheological characteristics of gum, OSP dispersions at concentrations
130 0.1, 0.3, 0.5, 0.7 and 1 % (w/v) were first prepared by dissolving of the required amount of dry
131 powdered gum in distilled water and gently stirred at room temperature for 2 h. The gum
132 dispersions were stored overnight at 5 °C to assure that the hydration of the polysaccharide was
133 complete.

134 Both steady shear viscosity and oscillatory shear tests were performed by Physica MCR 301
135 rheometer (Anton Paar GmbH, Graz, Austria) so that a concentric cylinder geometry (radius ratio
136 of 1.035) and a parallel plate geometry (25-mm diameter; 0.5-mm gap) were used for dilute
137 samples and concentrated dispersions, respectively. The temperature was adjusted to 25 °C with a
138 Viscotherm VT2 circulating bath and a controlled Peltier system (Anton Paar, GmbH) with an
139 accuracy of ± 0.01 °C.

140 Shear sweeps were conducted at 25 °C between 0.001 to 1000 s^{-1} so as to obtain flow curves. Flow
141 behavior of the dispersions were assessed by fitting the shear rate versus shear stress values to five
142 usual models, i.e., Newtonian ($\tau = m\dot{\gamma}$), Power-law ($\tau = m\dot{\gamma}^n$), Herschel-Bulkley ($\tau = m\dot{\gamma}^n + \tau_0$),
143 Bingham ($\tau = m\dot{\gamma} + \tau_0$), and Casson ($\sqrt{\tau} = m\sqrt{\dot{\gamma}} + \sqrt{\tau_0}$), Where τ is the shear stress (Pa), m is the
144 consistency coefficient (Pa.sn), $\dot{\gamma}$ is the shear rate ($1 s^{-1}$), the exponent n is flow behavior index
145 (dimensionless) and τ_0 is the yield stress (Pa) (Nejatian and Abbasi, 2019; Nejatian et al., 2018).

146 The effect of temperature on the flow properties was measured by performing shear sweeps for 1
147 % (w/v) OSP dispersion at 5 °C, 25 °C and 45 °C. Also, the temperature dependency of apparent
148 viscosity was evaluated by fitting the Arrhenius model ($\eta = \eta_0 \exp \frac{E_a}{RT}$) in which η_0 is the pre-
149 exponential factor (Pa.), E_a the activation energy for viscous flow (J/mol), R the universal gas
150 constant (8.314 J/mol K), and T the absolute temperature (K).

151 The 1 % (w/v) OSP gum dispersion was prepared for oscillatory shear measurements. Strain sweep
152 test was performed over the range 0.05–100 % at a fixed frequency (1 Hz) to determine the linear
153 viscoelastic region (LVR). Frequency sweep tests were also carried out at a wide range of
154 frequencies (0.01–20 Hz) and a constant strain (<LVR, ~ 0.5 %) to evaluate the dynamic
155 rheological properties (G' and G'').

156 In addition, the rheological behavior in response to the salt concentration (0.2 M) and type (NaCl
157 and CaCl₂) were determined just at a certain gum concentration, 1 % (w/v) and temperature, 25
158 °C.

159 *2.6 Statistical analysis*

160 All the measurements were made in triplicate and data were presented as mean \pm standard
161 deviation. Microsoft Excel Software (Microsoft Office, Package 2012) used for plotting the
162 rheological curves.

163 **3. Results and discussions**

164 *3.1. Compositional analysis*

165 The physicochemical and molecular parameters of the OSP are presented in Table 1. The results
166 showed the OSP contained 9.17% moisture, 1.88% ash, 2.14% of protein, 86.8% of total

167 carbohydrates, and DE of 79.68%. Plant's variety and growing conditions, extraction and
168 purification process are important factors affecting the chemical composition of hydrocolloids
169 (Razavi et al., 2014). Similar chemical composition for pectin extracted from sour oranges and the
170 total ash, moisture content, and protein content were 1.89, 8.81, and 1.45, respectively (Hosseini
171 et al., 2019).

172 Monosaccharides analysis using liquid chromatography (HPLC) showed that galacturonic acid
173 was the major component in OSP (~ 425 mg/g, about 85% of sugar composition). This was
174 followed by glucose (54 mg/g, about 10% of sugar composition). The wide diversity of
175 composition by acid and glucose indicates that OSP has rich pectin content but also some cellulose
176 or starch-like glucans. Such sugar composition was previously observed in the commercial low
177 methoxyl pectin (Peng et al., 2020) and some pectin from different food waste streams (Müller-
178 Maatsch et al., 2016). Also, minor quantities of fucose, galactose, arabinose, and rhamnose (about
179 4% of sugar composition) were also identified which can explain the complex polysaccharide
180 composition of OSP (Razavi et al., 2014). It has been reported that galactose, rhamnose, arabinose,
181 xylose and fucose are the principal neutral sugars found in pectin side chains (Hosseini et al.,
182 2019). Hydrocolloids with a higher amount of fucose, xylose, galacturonic acid, methoxyl groups,
183 and lower amounts of arabinose and nitrogenous fractions are reported to exhibit high viscosity
184 (Anderson and Grant, 1988). Similar observations were also reported by Balaghi et al. (2011) and
185 showed that tragacanth gums with a greater quantity of galacturonic acid and fucose exhibited
186 higher consistency coefficients (Balaghi et al., 2011). Similarly, Hosseini et al. (2019) observed
187 that galacturonic acid (65.3%) was the main monosaccharide of pectin extracted from sour orange
188 peels (Hosseini et al., 2019).

189 *3.2. Molecular weight parameters*

190 The results of molecular weights parameters are presented in Table 1. M_w (weight-average molar
191 mass), R_n (number average molar mass) and, R_z (z-average molar mass) for the OSP were 4511.8
192 (kDa), 61 (nm), and 61.1 (nm), respectively. The M_w measurement indicates a large M_w for OSP
193 confirming that such polysaccharides have a tendency to exhibit a higher viscous and pseudoplastic
194 properties when dissolved in water (Hosseini-Parvar et al., 2010). The high molecular weight of
195 OSP is similar to other hydrocolloids such as xanthan (4200 kDa), locust bean gum (50-3000 kDa),
196 Basil seed gum (1045-5980 kDa), guar (50-8000 kDa), psyllium (1500 kDa), and Karaya
197 (10,000 kDa) (Faria et al., 2011; Harding et al., 2017; Imeson, 2011; Milani and Maleki, 2012;
198 Naji-Tabasi et al., 2016). Different studies have shown that the pH of extraction may have an effect
199 on the molecular weight of pectin and pectin extracted in higher pH shows the higher M_w due to
200 the higher DE value of the pectin (Cho et al., 2019; Yapo et al., 2007). Using distilled water (pH=7)
201 to extract pectin from OSP, may explain the high M_w observed for the extracted pectin in this
202 research. Gavlighi and co-workers (2018) reported that the M_w of pectin extracted from
203 pomegranate peels depended on the extraction condition and the highest M_w and R_g observed for
204 the buffer extracted pectin ($18,631.85 \times 10^3$ g/mol and 102.80 nm) (Gavlighi et al., 2018).

205 *3.3. Rheological properties*

206 *3.3.1. Flow behavior*

207 Figure 1a compares the flow behavior of OSP dispersions within a concentration range of 0.1-1
208 wt%. On the basis of the highest determination coefficient (R^2) and the lowest root mean standard
209 error ($RMSE$), the flow behavior of all dispersions of OSP with different concentrations were
210 particularly nonlinear and best fitted to Power-law model ($\tau = m\dot{\gamma}^n$). The coefficients of evaluated
211 rheological models are shown in Table 2. The power law model has a wide application in food

212 industry and many studies have proved this model as the most appropriate model for flow behavior
213 study of the majority of food hydrocolloids (Khodaei et al., 2014).

214 The dependency of the apparent viscosity on the shear rate for the OSP dispersions in various
215 concentrations is shown in Figure 1b. As evident, the OSP dispersions indicated the typical
216 viscosity vs shear rate relationship of a colloidal food system including the polysaccharides
217 solutions. At lower shear rate (~ 0.1 1/s) and especially at higher gum concentrations (0.5-1 wt%),
218 the apparent viscosity was nearly independent of the shear rate. Indeed, when the shear rate is low,
219 the Brownian motion dominates the structural forces and favors the alignment of the elongated
220 coil along the flow direction. However, the viscosity reduced with increasing shear rate (shear
221 thinning behavior) arose from the equilibrium between the hydrodynamic forces and the structural
222 forces (Barnes, 2000; Windhab, 1995). In fact, above a critical shear rate, the deformation rate of
223 the gum chain entanglement due to the application of external forces becomes greater than the
224 formation rate of the new entanglement (Lapasin and Pricl, 1995).

225 As seen (Fig. 1b), the apparent viscosity decreased with reducing the gum concentration to 0.1%,
226 throughout the shear rate study. In addition, as the concentration of dispersion increases, the
227 intermolecular interactions increase and improve the viscosity. The positive effect of gum
228 concentration on the apparent viscosity can be also followed in Power law model parameters
229 (Table 1), so that with increasing in OSP concentration, the consistency coefficient (k) and flow
230 behavior index (n) increased and decreased, respectively. Generally, it seems that the apparent
231 viscosity of OSP is similar or even better than that of some other polysaccharides such as some
232 species of gum tragacanth (Balaghi et al., 2010), pectin (Marcotte et al., 2001), Persian gum
233 (Fadavi et al., 2014), guar gum (Kayacier and Dogan, 2006), carboxymethyl cellulose (Yasar et
234 al., 2007), etc.

235 Strain sweep dynamic rheological measurements showed that for OSP dispersion (1 wt%) storage
236 modulus (G') was somewhat higher than loss modulus (G'') (Fig. 2a). Nevertheless, the superiority
237 of each of these modules over the other in the frequency sweep test depended on the frequency.
238 As is evident in Fig. 2b, there was the transition from a predominantly viscous response at longer
239 time scales ($G'' > G'$) to a predominantly elastic response at shorter time scales ($G' > G''$), indicating
240 the dispersion has an entangled network structure. Such rheological behavior can be compared to
241 some gum tragacanth species (*Astragalus parrowianus* and *fluccosus*) (Balaghi et al., 2011) and
242 deacetylated *Sterculia striata* polysaccharide (De Brito et al., 2005).

243 3.3.2. Effect of salt and temperature on rheological properties

244 The Addition of salt (NaCl) to the OSP dispersion (1 wt%) decreased the apparent viscosity with
245 no changes in the reduction pattern or flow behavior (Fig. 3a). Moreover, the consistency
246 coefficient of 1 wt% OSP aqueous dispersion in the presence of 0.2 M NaCl decreased from 35.60
247 to 23.18 Pa.sⁿ while the flow behavior index remained almost unchanged (0.22 against 0.25). This
248 effect can be assigned to charge screening effect of the salt on long-range electrostatic repulsion
249 among the uronic acid residues of OSP (Balaghi et al., 2010). Based on strain sweep test, the salt
250 addition reduced amount of both G' and G'' , but the G' values in LVR were still greater than G''
251 (Fig. 2a). On the contrary to the NaCl-free OSP dispersion, the dispersion containing NaCl (0.2
252 M) indicated a crossover point at a high frequency (Fig. 2b). Furthermore, in the presence of NaCl,
253 the G' and G'' gap was larger. This suggests that NaCl caused a more drastic decrease in elastic
254 component than the viscous component. Interestingly, as is evident (Fig. 3a), incorporation of
255 CaCl₂ to OSP dispersion increased the viscosity which can be related to the bridging effect of Ca²⁺
256 forming a strong gel network of polysaccharide chains.

257 Figure 3b shows the temperature influence on the apparent viscosity of 1 wt% OSP dispersion as
258 a function of shear rate. As seen, the viscosity significantly declined by increasing in temperature
259 from 5 to 45 °C. This effect can be also observed in Power law model parameters so that by
260 increasing the temperature, the consistency coefficient decreased and the flow behavior index
261 increased (Table 3). However, the flow behavior index of the dispersion is still far from the typical
262 value of a Newtonian fluid (i.e., $n = 1$). In addition, the shear rate had a considerable effect on the
263 temperature dependence of OSP dispersion viscosity. Figure 3c shows the value of activation
264 energy obtained at two shear rates, 0.1 and 10 1/s for 1 wt% OSP aqueous dispersions. High R^2
265 values suggested that the apparent viscosity of dispersion in relation to temperature follows the
266 Arrhenius model. A higher flow E_a value at low rates of shear implicates more sensitivity of OSP
267 viscosity to temperature changes. This trend was also reported for other hydrocolloids such as
268 pectin (da Silva et al., 1994).

269

270 **4. Conclusion**

271 The compositional and rheological behavior of pectin extracted from bitter orange seeds (OSP) as
272 a novel source of high-quality pectin was evaluated in this study. Monosaccharides compositions
273 revealed that galacturonic acid was the major structure of pectin followed by glucose. Arabinose,
274 galactose, rhamnose, and fucose were also observed in smaller amounts and confirm the side chain
275 structure of the pectin. Molecular weight analysis of the pectin showed a high M_w of 4512 kDa.
276 OSP dispersions exhibited a non-Newtonian shear thinning behavior. Strain sweep dynamic
277 rheological measurements exhibited a higher storage modulus (G') than loss modulus (G'') and it
278 confirms the entangled structure of OSP. In conclusion, the mucilage extracted from orange seeds

279 is rich in pectin and demonstrates potential use as gelling or emulsion stabilizer in food
280 applications. Further studies to evaluate the functional properties and characterization of this novel
281 source of pectin is needed but if fully elucidated could potentially revolutionize the use of pectin
282 in the food industry.

283 **Conflict of interest**

284 All the authors declare no conflict of interest.

285 **Funding**

286 This research did not receive any specific grant from funding agencies in the public, commercial, or
287 not-for-profit sectors.

288 **Acknowledgement**

289 The authors would like to thank Dr. Edel McGarry for offering help in proofreading and language
290 editing of the manuscript.

291 **References**

292 Anderson, D., Grant, D. The chemical characterization of some Astragalus gum exudates. *Food*
293 *Hydrocoll.* **2**, 417-423 (1998)

294 AOAC, G. *Official methods of analysis of AOAC International*. Rockville, MD: AOAC
295 International, ISBN: 978-0-935584-87-5 (2016)

296 Asgari, K., Labbafi, M., Khodaiyan, F., Kazemi, M., Hosseini, S.S. Valorization of walnut
297 processing waste as a novel resource: Production and characterization of pectin. *J. Food Process.*
298 *Pres.* **44**, e14941 (2020)

299 Assoi, S., Konan, K., Agbo, G.N., Dodo, H., Holser, R., Wicker, L. Palmyra palm (*Borassus*
300 *aethiopum* Mart.) fruits: novel raw materials for the pectin industry. *J. Sci. Food Agric.* **97**, 2057-
301 2067 (2017)

- 302 Balaghi, S., Mohammadifar, M.A., Zargaraan, A. Physicochemical and rheological
303 characterization of gum tragacanth exudates from six species of Iranian Astragalus. *Food Biophys.*
304 **5**, 59-71 (2010)
- 305 Balaghi, S., Mohammadifar, M.A., Zargaraan, A., Gavlighi, H.A., Mohammadi, M. Compositional
306 analysis and rheological characterization of gum tragacanth exudates from six species of Iranian
307 Astragalus. *Food Hydrocoll.* **25**, 1775-1784 (2011)
- 308 Barnes, H.A. A handbook of elementary rheology. University of Wales, Institute of Non-
309 Newtonian Fluid Mechanics (2000)
- 310 Berk, Z. Citrus fruit processing. Academic press (2016)
- 311 Chaharbaghi, E., Khodaiyan, F., Hosseini, S.S. Optimization of pectin extraction from pistachio
312 green hull as a new source. *Carbohydr. Polym.* **173**, 107-113 (2017)
- 313 Chaliha, M., Williams, D., Smyth, H., Sultanbawa, Y. Extraction and characterization of a novel
314 Terminalia pectin. *Food Sci. Biotechnol.* **27**, 65-71 (2018)
- 315 Cho, E.-H., Jung, H.-T., Lee, B.-H., Kim, H.-S., Rhee, J.-K., Yoo, S.-H. Green process
316 development for apple-peel pectin production by organic acid extraction. *Carbohydr. Polym.* **204**,
317 97-103 (2019)
- 318 Christiaens, S., Van Buggenhout, S., Houben, K., Jamsazzadeh Kermani, Z., Moelants, K.R.,
319 Ngouemazong, E.D., Van Loey, A., Hendrickx, M.E. Process–structure–function relations of
320 pectin in food. *Crit. Rev. Food Sci. Nutr.* **56**, 1021-1042 (2016)
- 321 da Silva, J.L., Gonçalves, M., Rao, M. Influence of temperature on the dynamic and steady-shear
322 rheology of pectin dispersions. *Carbohydr. Polym.* **23**, 77-87 (1994)
- 323 De Brito, A.C.F., Sierakowski, M.R., Reicher, F., Feitosa, J.P., De Paula, R.C.M. Dynamic
324 rheological study of Sterculia striata and karaya polysaccharides in aqueous solution. *Food*
325 *Hydrocoll.* **19**, 861-867 (2005)
- 326 Fadavi, G., Mohammadifar, M.A., Zargarran, A., Mortazavian, A.M., Komeili, R. Composition
327 and physicochemical properties of Zedo gum exudates from Amygdalus scoparia. *Carbohydrate*
328 *polymers.* **101**, 1074-1080 (2014)
- 329 Faria, S., de Oliveira Petkowicz, C.L., De Moraes, S.A.L., Terrones, M.G.H., De Resende, M.M.,
330 de Franca, F.P., Cardoso, V.L. Characterization of xanthan gum produced from sugar cane broth.
331 *Carbohydr. Polym.* **86**, 469-476 (2011)
- 332 Gavlighi, H.A., Meyer, A.S., Zaidel, D.N.A., Mohammadifar, M.A., Mikkelsen, J.D. Stabilization
333 of emulsions by gum tragacanth (*Astragalus* spp.) correlates to the galacturonic acid content and
334 methoxylation degree of the gum. *Food Hydrocoll.* **31**, 5-14 (2013)

- 335 Gavlighi, H.A., Tabarsa, M., You, S., Surayot, U., Ghaderi-Ghahfarokhi, M. Extraction,
336 characterization and immunomodulatory property of pectic polysaccharide from pomegranate
337 peels: Enzymatic vs conventional approach. *Int. J. Biol. Macromol.* **116**, 698-706 (2018)
- 338 Gharibzahedi, S.M.T., Smith, B., Guo, Y. Ultrasound-microwave assisted extraction of pectin
339 from fig (*Ficus carica* L.) skin: Optimization, characterization and bioactivity. *Carbohydr. Polym.*
340 **222**, 114992 (2019)
- 341 Harding, S.E., Tombs, M.P., Adams, G.G., Paulsen, B.S., Inngjerdingen, K.T., Barsett, H. An
342 introduction to polysaccharide biotechnology. CRC Press (2017)
- 343 Hosseini-Parvar, S., Matia-Merino, L., Goh, K., Razavi, S.M.A., Mortazavi, S.A. Steady shear
344 flow behavior of gum extracted from *Ocimum basilicum* L. seed: Effect of concentration and
345 temperature. *J. Food Eng.* **101**, 236-243 (2010)
- 346 Hosseini, S.S., Khodaiyan, F., Kazemi, M., Najari, Z. Optimization and characterization of pectin
347 extracted from sour orange peel by ultrasound assisted method. *Int. J. Biol. Macromol.* **125**, 621-
348 629 (2019)
- 349 Hosseini, S.S., Khodaiyan, F., Yarmand, M.S. Aqueous extraction of pectin from sour orange peel
350 and its preliminary physicochemical properties. *Int. J. Biol. Macromol.* **82**, 920-926 (2016)
- 351 Imeson, A. Food stabilisers, thickeners and gelling agents. John Wiley & Sons (2011)
- 352 Kayacier, A., Dogan, M. Rheological properties of some gums-salep mixed solutions. *J. Food Eng.*
353 **72**, 261-265 (2006)
- 354 Khodaei, D., Razavi, S.M., Khodaparast, M.H. Functional properties of Balangu seed gum over
355 multiple freeze–thaw cycles. *Food Res. Int.* **66**, 58-68 (2014)
- 356 Lapasin, R., Prich, S. Rheology of polysaccharide systems, in: Lapasin, R. (Ed.), *Rheology of*
357 *industrial polysaccharides: Theory and applications*. Springer, pp. 250-494 (1005)
- 358 Löfgren, C., Hermansson, A.-M. Synergistic rheological behaviour of mixed HM/LM pectin gels.
359 *Food hydrocoll.* **21**, 480-486 (2007)
- 360 Marcotte, M., Taherian Hoshahili, A.R., Ramaswamy, H.S. Rheological properties of selected
361 hydrocolloids as a function of concentration and temperature. *Food Res. Int.* **34**, 695-703 (2001)
- 362 Maxwell, E.G., Belshaw, N.J., Waldron, K.W., Morris, V.J. Pectin—an emerging new bioactive
363 food polysaccharide. *Trends Food Sci. Technol.* **24**, 64-73 (2012)
- 364 May, C.D. Industrial pectins: sources, production and applications. *Carbohydr. Polym.* **12**, 79-99
365 (1990)
- 366 Milani, J., Maleki, G. Hydrocolloids in food industry. In Valdez, B. (Ed.), *Food industrial*
367 *processes—Methods and equipment*. 2, 2-37. IntechOpen, ISBN: 978-953-51-4352-9 (2012)

- 368 Moufida, S.d., Marzouk, B. Biochemical characterization of blood orange, sweet orange, lemon,
369 bergamot and bitter orange. *Phytochemistry*. **62**, 1283-1289 (2003)
- 370 Müller-Maatsch, J., Bencivenni, M., Caligiani, A., Tedeschi, T., Bruggeman, G., Bosch, M.,
371 Petrusan, J., Van Droogenbroeck, B., Elst, K., Sforza, S. Pectin content and composition from
372 different food waste streams. *Food Chem.* **201**, 37-45 (2016)
- 373 Naji-Tabasi, S., Razavi, S.M.A., Mohebbi, M., Malaekheh-Nikouei, B. New studies on basil
374 (*Ocimum bacilicum* L.) seed gum: Part I–Fractionation, physicochemical and surface activity
375 characterization. *Food Hydrocoll.* **52**, 350-358 (2016)
- 376 Nejatian, M., Abbasi, S. Formation of concentrated triglyceride nanoemulsions and nanogels:
377 natural emulsifiers and high power ultrasound. *RSC Adv.* **9**, 28330-28344 (2019)
- 378 Nejatian, M., Abbasi, S., Azarikia, F. Gum Tragacanth: Structure, characteristics and applications
379 in foods. *Int. J. Biol. Macromol.* **160**, 846-860 (2020)
- 380 Nejatian, M., Abbasi, S., Kadkhodae, R. Ultrasonic-Assisted Fabrication of Concentrated
381 Triglyceride Nanoemulsions and Nanogels. *Langmuir*, **34**, 11433-11441 (2018)
- 382 Peng, X., Yang, G., Shi, Y., Zhou, Y., Zhang, M., Li, S. Box–Behnken design based statistical
383 modeling for the extraction and physicochemical properties of pectin from sunflower heads and
384 the comparison with commercial low-methoxyl pectin. *Sci. Rep.* **10**, 3595 (2020)
- 385 Razavi, S.M.A., Cui, S.W., Guo, Q., Ding, H. Some physicochemical properties of sage (*Salvia*
386 *macrospion*) seed gum. *Food Hydrocoll.* **35**, 453-462 (2014)
- 387 Rincón, F., Muñoz, J., Ramírez, P., Galán, H., Alfaro, M.C. Physicochemical and rheological
388 characterization of *Prosopis juliflora* seed gum aqueous dispersions. *Food Hydrocoll.* **35**, 348-357
389 (2014)
- 390 Shan, Y. Comprehensive utilization of citrus by-products. Academic Press (2016)
- 391 Windhab, E. Rheology in food processing, in: Beckett, S.T. (Ed.), *Physico-chemical aspects of*
392 *food processing*. Springer, pp. 80-116 (1995)
- 393 Yapo, B., Robert, C., Etienne, I., Wathelet, B., Paquot, M. Effect of extraction conditions on the
394 yield, purity and surface properties of sugar beet pulp pectin extracts. *Food chem.* **100**, 1356-1364
395 (2007)
- 396 Yasar, F., Togrul, H., Arslan, N. Flow properties of cellulose and carboxymethyl cellulose from
397 orange peel. *J. Food Eng.* **81**, 187-199 (2007)
- 398 Zibae, E., Kamalian, S., Tajvar, M., Amiri, M.S., Ramezani, M., Moghadam, A.T., Emami, S.A.,
399 Sahebkar, A. Citrus species: A Review of Traditional Uses, Phytochemistry and Pharmacology.
400 *Curr. Pharm. Des.* **26**, 44-97 (2020)

401

Table 1. Composition and molecular parameters of Bitter orange seed pectin (OSP)

Composition	
Moisture (%)	9.17 ± 0.37
Total ash (%)	1.88 ± 0.19
Total proteins (%)	2.14 ± 0.2
Total carbohydrates (%)	86.82 ± 0.33
DE (%)	79.68 ± 0.65
Monosaccharides (mg/g):	
Galacturonic Acid	424.99
Glucose	54.10
Rhamnose	8.37
Arabinose	5.54
Galactose	4.83
Fucose	1.78
M _w (kDa)	4511.75 ± 135.65
R _n (nm)	61 ± 0.8
R _z (nm)	61.1 ± 0.9

DE (Degree of esterification) M_n (number average molar mass), M_w (weight average molar mass) and M_z (z-average molar mass)

Table 2. Flow behavior of OSP dispersions (0.1-1% w/v) fitted to rheological models.

Rheological models and variables	Concentration (% w/v)				
	0.1	0.3	0.5	0.7	1
Newtonian					
K (Pa s ⁿ)	0.008	0.019	0.043	0.070	
R ²	0.98	0.85	0.60	0.41	0.00
RMSE	0.252	1.607	5.937	11.740	
Power law					
K (Pa s ⁿ)	0.005	0.490	3.068	7.206	35.6
n	1.05	0.504	0.348	0.290	0.219
R ²	0.98	1 (0.998)	1(0.992)	0.98	0.97
RMSE	0.259	0.151	0.798	1.869	8.314
Herschel–Bulkely					
K (Pa s ⁿ)	0.003				
n	1.11				
τ_0 (Pa)	0.113				
R ²	0.98	-*	-*	-*	-*
RMSE	0.250				
Bingham					
K (Pa s ⁿ)	0.008	0.018	0.037	0.057	0.156
τ_0 (Pa)	0.051	0.900	3.762	7.961	36.300
R ²	0.98	0.89	0.74	0.64	0.49
RMSE	0.259	1.39	4.846	9.192	33.720
Casson					
K (Pa s ⁿ)	0.441	3.93	26.470	78.750	925.600
τ_0 (Pa)	2.22×10^{-14}	2.22×10^{-14}	2.22×10^{-14}	3.62×10^{-14}	3.37×10^{-13}
R ²	0.84	0.84	0.94	0.97	0.96
RMSE	1.667	1.667	2.161	2.423	9.478

* Data fitting to Herschel–Bulkely and Bingham models for these samples indicated negative values of yield stress, so the obtained results for these two models in such samples were not reliable.

Table 3. Power law parameters and flow activation energy for OSP (1 % w/v) dispersion at different temperatures.

Temperature (°C)	Power law parameters			
	<i>K</i> (Pa.s ^{<i>n</i>})	<i>n</i>	<i>R</i> ²	<i>RMES</i>
5	43.51	0.188	0.94	11.03
25	35.6	0.219	0.97	8.31
45	19.39	0.252	0.97	5.40

Figure 1. Comparison of the flow curves (a) and influence of shear rate on apparent viscosity of the OSP dispersions in different concentrations [0.1 wt% (◆), 0.3 wt% (■), 0.5 wt% (▲), 0.7 wt% (●), 1 wt%(✱)]

Figure 2. Comparison of the dependency of G' (filled) and G'' (hollow) on (a) strain and (b) frequency for 1 wt% OSP dispersions in the absence (□, ■) and presence (○, ●) of added NaCl (0.2 M).

Figure 3. Effect of salts (a; 0 wt% (●), 0.2 M NaCl (▲) and 0.2 M CaCl₂ (■) and temperature (b: 5 °C (□), 25 °C (○) and 45 °C (△) on the apparent viscosity of 1 wt% OSP dispersion as a function of shear rate. Arrhenius plots (c) at shear rate of 0.1 1/s (■) and 10 1/s (□) for 1 wt% OSP dispersions.

Figure 1.

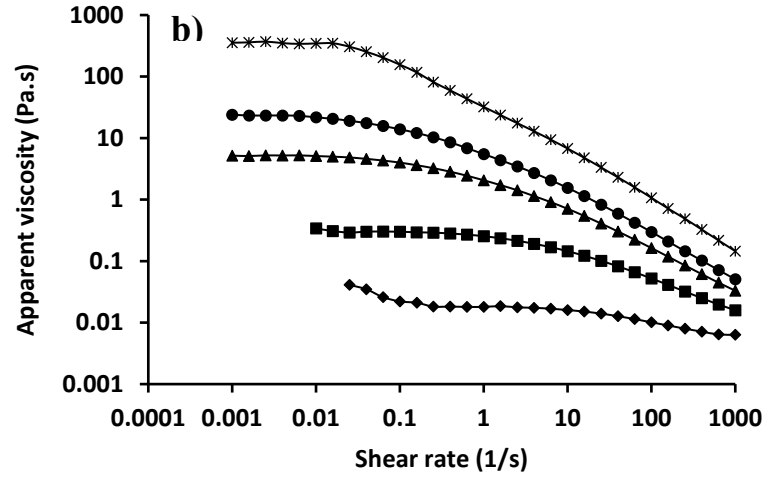
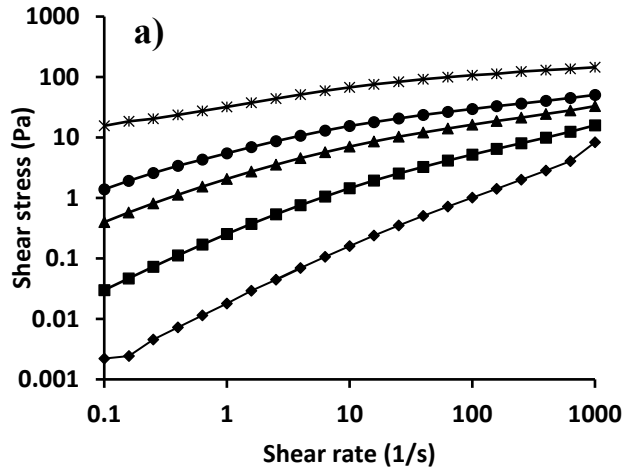


Figure 2.

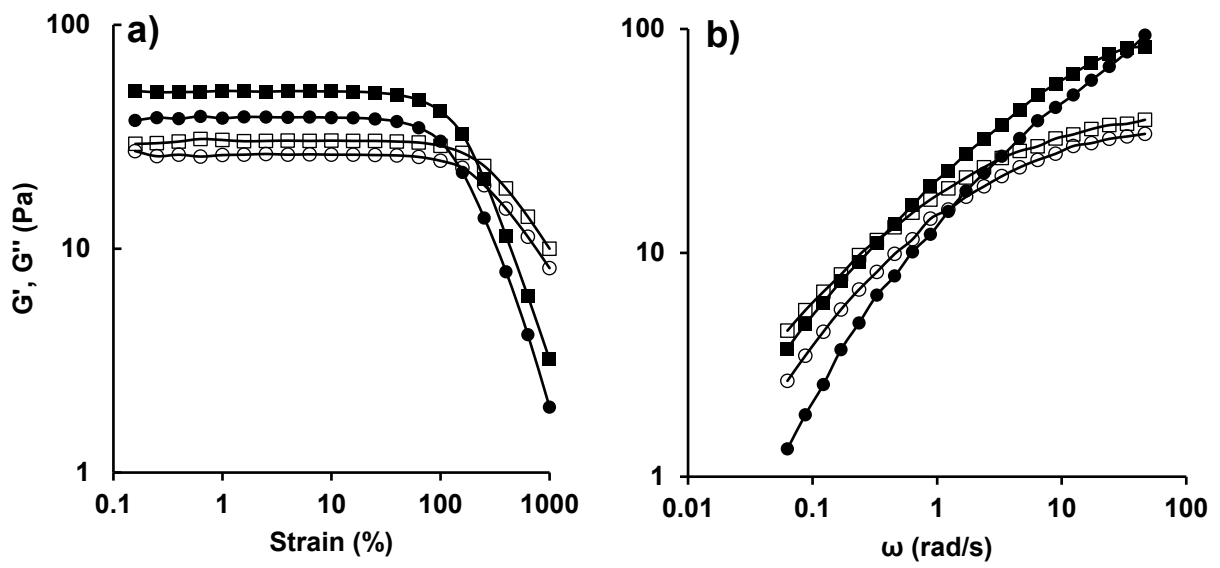


Figure 3.

